Electronic supplementary information

Two-dimensional MBenes with ordered metal vacancies for surface-enhanced Raman scattering

Leilei Lan[a,b], Xingce Fan[b], Caiye Zhao[a], Juan Gao[a], Zhongwei Qu[a], Wenzhe Song[b], Haorun Yao[b], Mingze Li[b], and Teng Qiu*[b,c]

[a] School of Mechanics and Optoelectronic Physics, Anhui University of Science and Technology, Huainan 232001, China

[b] School of Physics, Southeast University, Nanjing 211189, China

[c] Center for Flexible RF Technology, Frontiers Science Center for Mobile Information Communication and Security, Southeast University, Nanjing 210096, China

* E-mail: tqiu@seu.edu.cn.

Section S1: Calculation of the enhancement factor (EF)

The EF of the samples could be estimated using the equation below:[1]

$EF = (I_{SERS}/N_{SERS}) / (I_{bulk}/N_{bulk})$ (S1)

$N_{SERS} = CVN_A A_{Raman}/A_{Sub}$ (S2)

$Nbulk = \rho h A_{Raman} N_A/M$ (S3)

where I_{SERS} and I_{bulk} are the intensities of the selected Raman peak in the SERS and non-SERS spectra, respectively. N_{SERS} and N_{bulk} are the average number of molecules in scattering area for SERS and non-SERS measurement. The data of bulk R6G is used as non-SERS-active reference. C is the molar concentration of R6G solution and V is the volume of the droplet (20 μL). N_A is Avogadro constant (6.023×10^{23} mol^{-1}). A_{Raman} is the laser spot area. A_{Sub} is the effective area of the substrate, which is approximately 9 πmm^2. The confocal depth h of the laser beam is 21 μm. The molecular weight M of R6G is 479 g mol^{-1} and density ρ of bulk R6G is 1.15 g cm^{-3}.

Section S2: Calculation of the degree of charge transfer

The degree of charge transfer ($P_{CT}(k)$) is used for investigating the charge transfer (CT) contributions to the SERS intensity, which can be described as follow formula:[2,3]

$P_{CT}(k) = (I^k(CT)-I^k(SPR)) / (I^k(CT)+I^0(SPR))$ (S4)

where $I^k(CT)$ is the Raman intensity of a band in which the CT contributes to the intensity of enhanced Raman signals. Two bands with no CT contribution are selected as a reference. One is $I^0(SPR)$, the intensity of the totally symmetric band only comes from the contribution of the surface plasmon resonance (SPR). The other is called $I^k(SPR)$. If the k band is totally symmetric vibration band, the main contribution to the intensity arises from the SPR, and $I^k(SPR)$ =

I^0(SPR). If k band is non-totally symmetric vibration band, the contribution from CT dominates the intensity. At this moment, I^k(SPR) is usually quite small, and it can be assumed to be zero in many cases. It can be seen from formula that when P_{CT} is zero, there are no CT contributions; when P_{CT} close to 1, the CT contributions will dominate the spectrum. We could select the totally symmetric 1360 cm^{-1} mode and the non-totally symmetric 612 cm^{-1} mode as line 0 and k, respectively.[4] Ignoring the adsorption behavior of molecules, the degree of CT for R6G (1×10^{-6} M) on 2D $Mo_{4/3}B_2$ is 0.64, which demonstrates that the chemical mechanism is the main enhancement mechanism.

Section S3: Figures

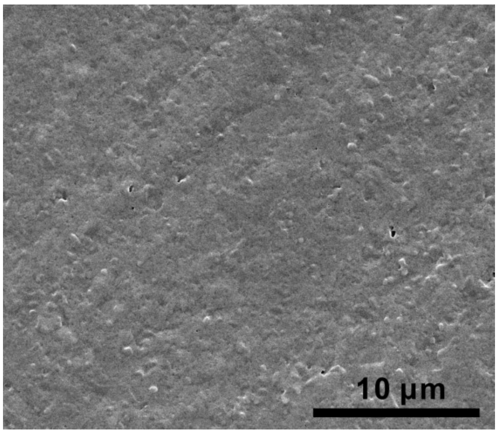

Fig. S1 Low-magnification SEM image of 2D $Mo_{4/3}B_2$ dispersion deposited on Si substrate.

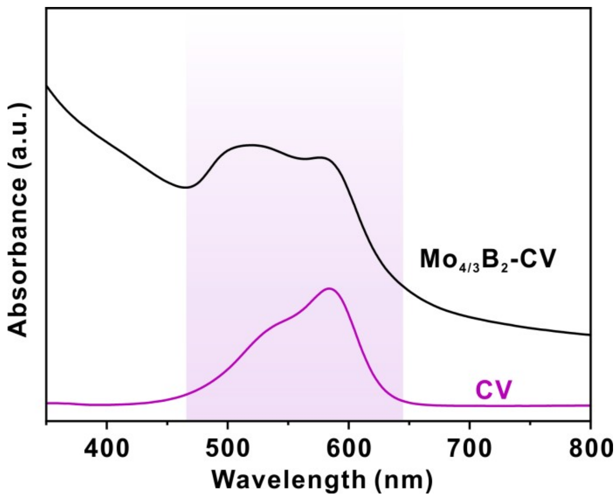

Fig. S2 UV-vis absorption spectra of CV molecule and $Mo_{4/3}B_2$-CV.

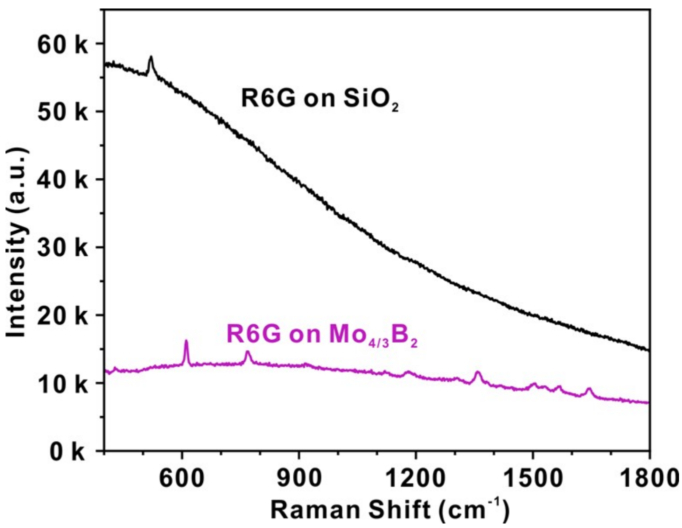

Fig. S3 Raman spectra of R6G (1×10^{-6} M) adsorbed on SiO_2 (reference sample) and 2D $Mo_{4/3}B_2$ MBene substrate. Both of the two spectra are pristine without baseline correction.

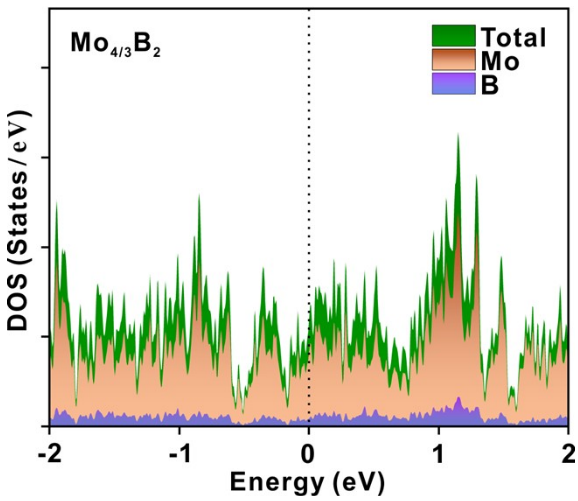

Fig. S4 The DFT calculations of the DOS of 2D $Mo_{4/3}B_2$.

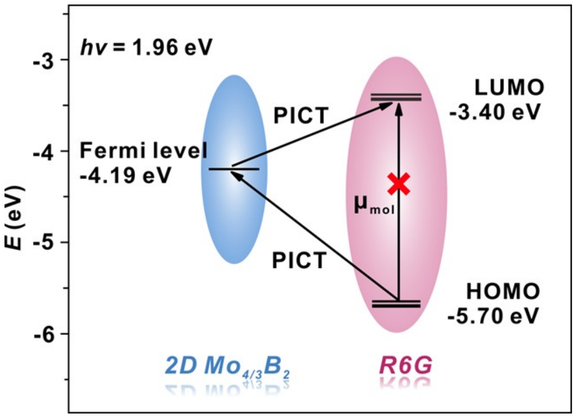

Fig. S5 The schematic energy level diagram of R6G-$Mo_{4/3}B_2$ system under the illumination of 633 nm (1.96 eV).

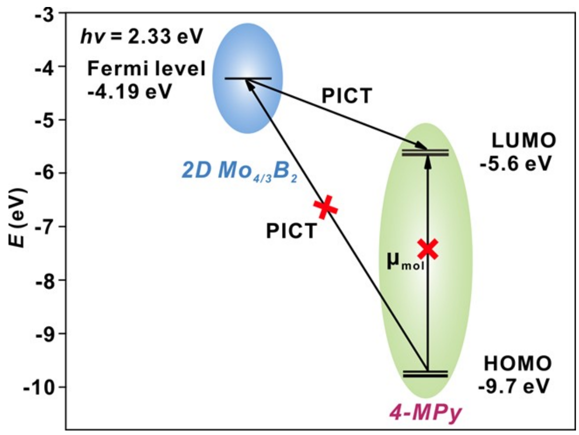

Fig. S6 The schematic energy level diagram of 4-MPy-$Mo_{4/3}B_2$ system under the illumination of 532 nm (2.33 eV).

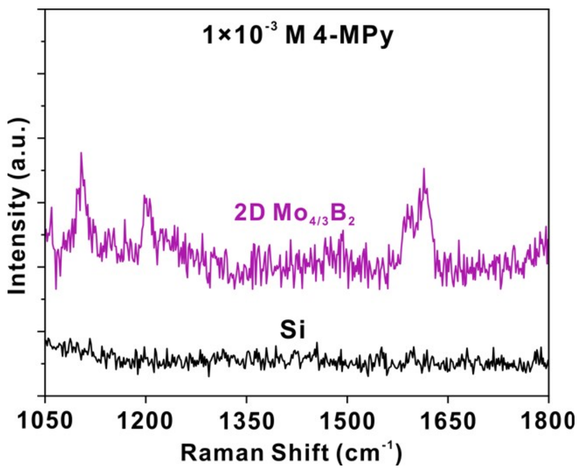

Fig. S7 Raman spectra of 4-MPy (1×10^{-3} M) adsorbed on the 2D $Mo_{4/3}B_2$ and Si substrates.

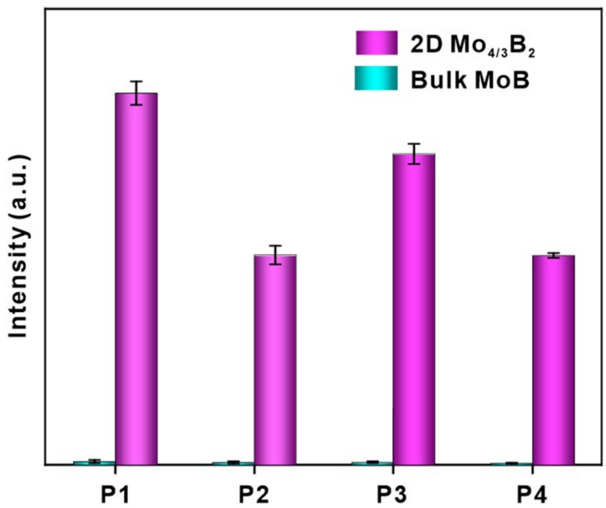

Fig. S8 The intensity columns of R6G (1×10^{-4} M) adsorbed on bulk MoB and 2D $Mo_{4/3}B_2$.

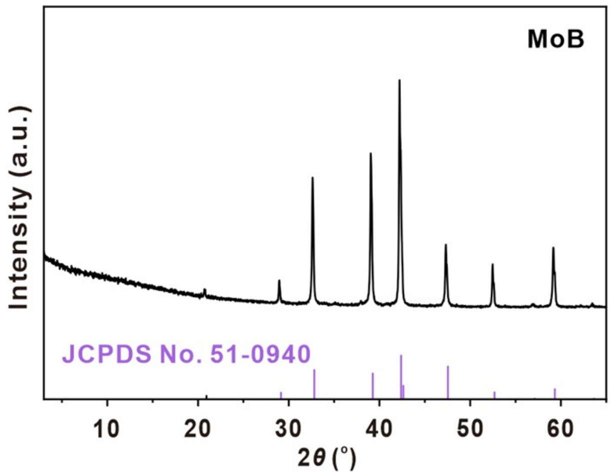

Fig. S9 The XRD pattern of commercial bulk MoB.

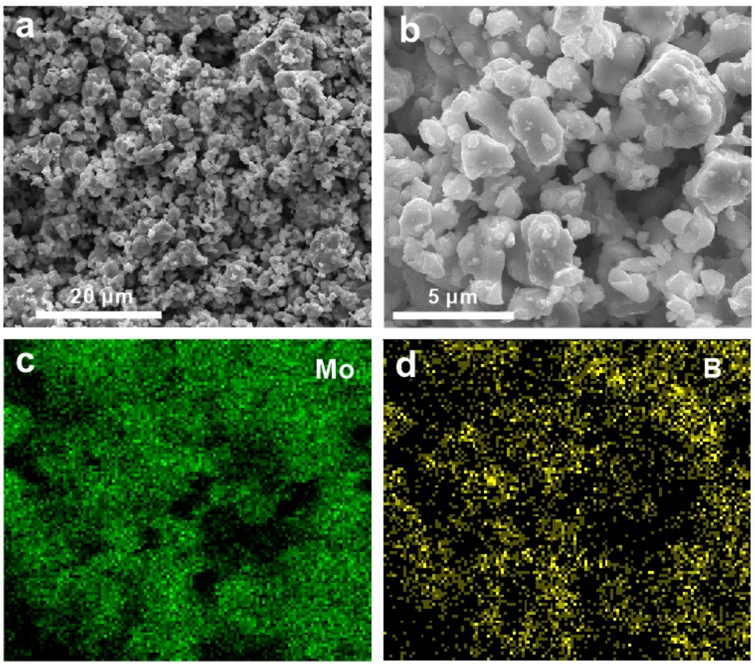

Fig. S10 (a, b) SEM images of commercial bulk MoB. (c, d) The corresponding elemental mapping images of commercial bulk MoB.

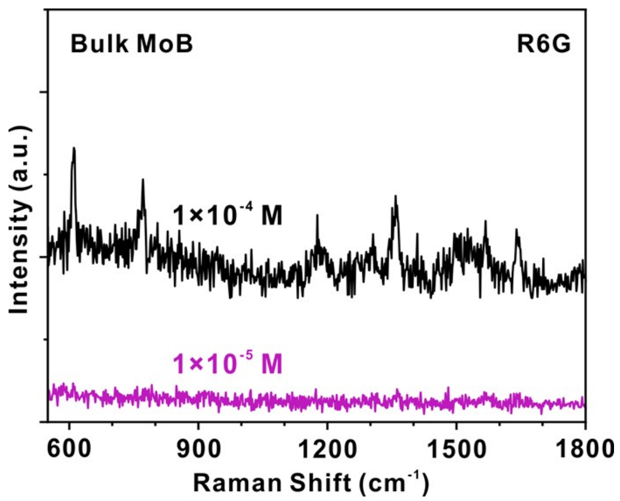

Fig. S11 Raman spectra of R6G with different concentrations adsorbed on the bulk MoB.

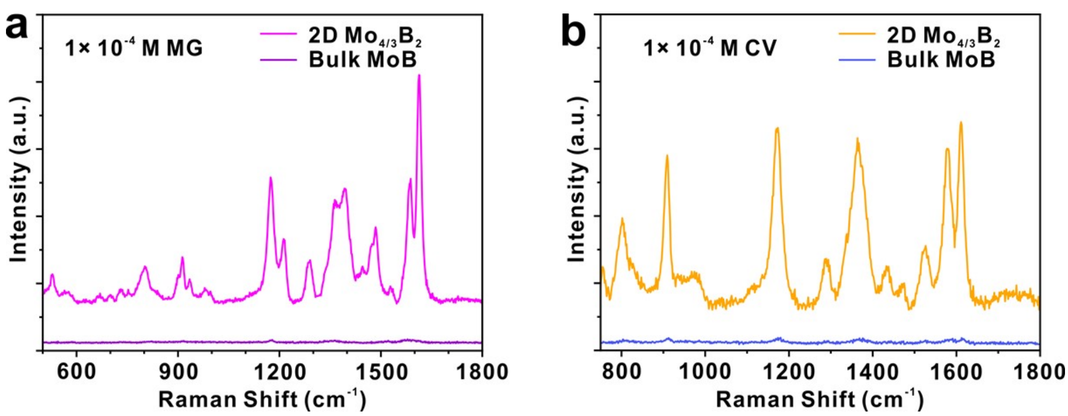

Fig. S12 Raman spectra of (a) MG and (b) CV molecules (1 × 10^{-4} M) adsorbed on bulk MoB and 2D $Mo_{4/3}B_2$.

Section S4: Tables

Table S1. Comparison of the SERS sensitivity of various noble-metal-free materials.

SERS Substrate	Analyte	Detection limit (mol/L)	Enhancement factor	Ref.
MoO_2 nanodumbbells	R6G	10^{-7}	3.75×10^6	5
Cu_2O superstructure particles	R6G	10^{-9}	8×10^5	6
ZnO superstructure particles	4-Mpy	-	10^5	7
Rare-earth nanosheets	R6G	10^{-12}	9.1×10^8	8
Amorphous TiO_2 nanosheets	4-MBA	-	1.86×10^6	9
Ta_2C MXene	MV	10^{-7}	1.4×10^6	10
Ta_2O_5 nanorods	R6G	9×10^{-9}	2.2×10^7	11
Graphene	R6G	8×10^{-10}	-	12
MOFs materials	R6G	10^{-8}	10^6	13
Atomically thin $TaSe_2$ film	R6G	10^{-10}	1.5×10^5	14
DFP-4T organic semiconductor films	MB	10^{-8}	10^5	15
2D $PdSe_2$	R6G	10^{-9}	10^5	16
2D borocarbonitride nanosheets	R6G	10^{-8}	5.34×10^5	17
$Mo_{4/3}B_2$ MBene	**R6G**	**1×10^{-9}**	**3.88×10^6**	**This work**

References

1 S. Cong,Y. Y. Yuan, Z. G. Chen, J. Y. Hou, M. Yang, Y. L. Su, Y. Y. Zhang, L. Li, Q. W. Li, F. X. Geng and Z. G. Zhao, *Nat. Commun.*, 2015, **6**, 7800.

2 M. V. Canamares, C. Chenal, R. L. Birke and J. R. Lombardi, *J. Phys. Chem. C*, 2008, **112**, 20295−20300.

3 J. R. Lombardi, R. L. Birke and C. Chenal, *ChemPhysChem*, 2008, **9**, 1617−1623.

4 M. Z. Li, Y. J. Wei, X. C. Fan, G. Q. Li, Q. Hao and T. Qiu, *Nano Res.*, 2022, **15**, 637−643.

5 Q. Q. Zhang, X. S. Li, Q. Ma, Q. Zhang, H. Bai, W. C. Yi, J. Y. Liu, J. Han and G. C. Xi, *Nat. Commun.*, 2017, **8**, 14903.

6 J. Lin, Y. Shang, X. X. Li, J. Yu, X. T. Wang and L. Guo, *Adv. Mater.*, 2017, **29**, 1604797.

7 W. Ji, L. F. Li, W. Song, X. N. Wang, B. Zhao and Y. Ozaki, *Angew. Chem. Int. Ed.*, 2019, **58**, 14452−14456.

8 J. B. Li, W. C. Yi, M. Yin, H. F. Yang, J. F. Li, Y. H. Li, Z. W. Jiao, H. Bai, M. Q. Zou and G. C. Xi, *ACS Nano*, 2022, **16**, 1160−1169.

9 X. T. Wang, W. X. Shi, S. X. Wang, H. W. Zhao, J. Lin, Z. Yang, M. Chen and L. Guo, *J. Am. Chem. Soc.,* 2019, **141**, 5856−5862.

10 Y. S. Peng, C. L. Lin, L. Long, T. Masaki, M. Tang, L. L. Yang, J. J. Liu, Z. R. Huang, Z. Y. Li, X. Y. Luo, J. R. Lombardi and Y. Yang, *Nano-Micro Lett.*, 2021, **13**, 52.

11 L. L. Yang, Y. S. Peng, Y. Yang, J. J. Liu, H. L. Huang, B. H. Yu, J. M. Zhao, Y. L. Lu, Z. R. Huang, Z. Y. Li and J. R. Lombardi, *Adv. Sci.*, 2019, **6**, 1900310.

12 X. Ling, L. M. Xie, Y. Fang, H. Xu, H. L. Zhang, J. Kong, M. Dresselhaus, J. Zhang and Z. F. Liu, *Nano Lett.*, 2010, **10**, 553−561.

13 H. Z. Sun, S. Cong, Z. H. Zheng, Z. Wang, Z. G. Chen and Z. G. Zhao, *J. Am. Chem. Soc.*, 2019, **141**, 870−878.

14 Y. C. Ge, F. Wang, Y. Yang, Y. Xu, Y. Ye, Y. Cai, Q. W. Zhang, S. Y. Cai, D. F. Jiang, X. H. Liu, B. Liedberg, J. Mao and Y. Wang, *Small*, 2022, **18**, 2107027.

15 G. Demirel, R. L. M. Gieseking, R. Ozdemir, S. Kahmann, M. A. Loi, G. C. Schatz, A. Facchetti and H. Usta, *Nat. Commun.*, 2019, **10**, 5502.

16 Z. H. Lei, X. K. Zhang, Y. Zhao, A. X. Wei, L. L. Tao, Y. B. Yang, Z. Q. Zheng, L. Tao, P. Yu and J. B. Li, *Nanoscale*, 2022, **14**, 4181−4181.

17 C. Liang, Z. A. Lu, M. Zheng, M. X. Chen, Y. Y. Zhang, B. Zhang, J. X. Zhang and P. Xu, *Nano Lett.*, 2022, **22**, 6590−6598.